Eur. Phys. J. A **17**, 241–244 (2003)
DOI 10.1140/epja/i2002-10153-2

THE EUROPEAN PHYSICAL JOURNAL A

First measurement of the helicity-dependent $\vec{\gamma}\vec{p} \to p\eta$ differential cross-section

The GDH and A2 Collaborations

J. Ahrens[9], S. Altieri[15,16], J.R.M. Annand[6], G. Anton[3], H.-J. Arends[9,a], K. Aulenbacher[9], R. Beck[9], C. Bradtke[1], A. Braghieri[15], N. d'Hose[5], D. Drechsel[9], H. Dutz[2], S. Goertz[1], P. Grabmayr[17], K. Hansen[8], J. Harmsen[1], D. von Harrach[9], S. Hasegawa[13], T. Hasegawa[11], E. Heid[9], K. Helbing[3], H. Holvoet[4], L. Van Hoorebeke[4], N. Horikawa[14], T. Iwata[13,b], O. Jahn[9], P. Jennewein[9], T. Kageya[14], B. Kiel[3], F. Klein[2], R. Kondratiev[12], K. Kossert[7], J. Krimmer[17], M. Lang[9], B. Lannoy[4], R. Leukel[9], V. Lisin[12], T. Matsuda[11], J.C. McGeorge[6], A. Meier[1], D. Menze[2], W. Meyer[1], T. Michel[3], J. Naumann[3], A. Panzeri[15,16], P. Pedroni[15], T. Pinelli[15,16], I. Preobrajenski[9,12], E. Radtke[1], E. Reichert[10], G. Reicherz[1], Ch. Rohlof[2], G. Rosner[6], D. Ryckbosch[4], M. Sauer[17], B. Schoch[2], M. Schumacher[7], B. Seitz[7,c], T. Speckner[3], N. Takabayashi[13], G. Tamas[9], A. Thomas[9], R. van de Vyver[4], A. Wakai[14], W. Weihofen[7], F. Wissmann[7], F. Zapadtka[7], and G. Zeitler[3]

[1] Institut für Experimentalphysik, Ruhr-Universität Bochum, D-44801 Bochum, Germany
[2] Physikalisches Institut, Universität Bonn, D-53115 Bonn, Germany
[3] Physikalisches Institut, Universität Erlangen-Nürnberg, D-91058 Erlangen, Germany
[4] Subatomaire en Stralingsfysica, Universiteit Gent, B-9000 Gent, Belgium
[5] CEA Saclay, DSM/DAPNIA/SPhN, F-91191 Gif-sur-Yvette Cedex, France
[6] Department of Physics & Astronomy, University of Glasgow, Glasgow G12 8QQ, UK
[7] II. Physikalisches Institut, Universität Göttingen, D-37073 Göttingen, Germany
[8] Department of Physics, University of Lund, Lund, Sweden
[9] Institut für Kernphysik, Universität Mainz, D-55099 Mainz, Germany
[10] Institut für Physik, Universität Mainz, D-55099 Mainz, Germany
[11] Faculty of Engineering, Miyazaki University, Miyazaki, Japan
[12] INR, Academy of Science, Moscow, Russia
[13] Department of Physics, Nagoya University, Chikusa-ku, Nagoya, Japan
[14] CIRSE, Nagoya University, Chikusa-ku, Nagoya, Japan
[15] INFN, Sezione di Pavia, I-27100 Pavia, Italy
[16] Dipartimento di Fisica Nucleare e Teorica, Università di Pavia, I-27100 Pavia, Italy
[17] Physikalisches Institut, Universität Tübingen, D-72076 Tübingen, Germany

Received: 19 December 2002 /
Published online: 20 May 2003 –
Communicated by Th. Wacher

Abstract. The helicity dependence of the $\vec{\gamma}\vec{p} \to p\eta$ reaction has been measured for the first time at a center-of-mass angle $\theta^*_\eta = 70°$ in the photon energy range from 780 MeV to 790 MeV. The experiment, performed at the Mainz microtron MAMI, used a 4π-detector system, a circularly polarized, tagged photon beam, and a longitudinally polarized frozen-spin target. The helicity 3/2 cross-section is found to be small and the results for helicity 1/2 agree with predictions from the MAID analysis.

PACS. 13.60.Le Meson production – 14.20.Gk Baryon resonances with $S = 0$ – 25.20.Lj Photoproduction reactions

1 Introduction

Over many years, experimental and theoretical studies of nucleon resonances have been performed using meson reactions, mainly pion-induced reactions and pion photoproduction processes. Recently, a number of experimental and theoretical advances in the study of η photoproduction have taken place. New experiments have been performed at MAMI (Mainz) [1], ELSA (Bonn) [2], GRAAL [3], and JLab [4], while, on the theoretical side, different models have been developed such as effective Lagrangian approaches [5,6], coupled-channel calculations [7], generalized Lee model calculations [8], constituent quark

[a] e-mail: `arends@kph.uni-mainz.de`
[b] *Present address*: Department of Physics, Yamagata University, Yamagata 990-8560, Japan.
[c] *Present address*: II. Physikalisches Institut, Universität Gießen, Gießen, Germany.

models [9], and $SU(3)$ chiral meson-baryon Lagrangian theories [10,11].

From all these studies it became clear that, near threshold, the $S_{11}(1535)$-resonance plays a dominant role in η production that is analogous to the role of the $\Delta(1232)$-resonance in pion production, while the contribution of all the other resonances (such as $D_{13}(1520)$, $S_{11}(1650)$ or $P_{11}(1440)$) is very small.

As pointed out in refs. [12,13], polarization observables are a powerful tool to disentangle the contributions of small resonances in η photoproduction. Data on the polarized-target asymmetry (from Bonn) and on the polarized photon beam asymmetry (from GRAAL) are available but no double-polarization observable has been measured up to now. As an introductory step in this study, we present in this article the first measurement of the helicity-dependent differential cross-section of the $\vec{\gamma}\vec{p} \to p\eta$ reaction near threshold. These data were obtained during the GDH experiment [14,15] at the Mainz microtron MAMI, which studied the helicity structure of the exclusive and inclusive photoproduction cross-sections and their contributions to the Gerasimov-Drell-Hearn sum rule. Since the S-waves have only helicity 1/2 contributions, a separation of the helicity 1/2 and 3/2 terms is very interesting in order to investigate background and higher resonance contributions.

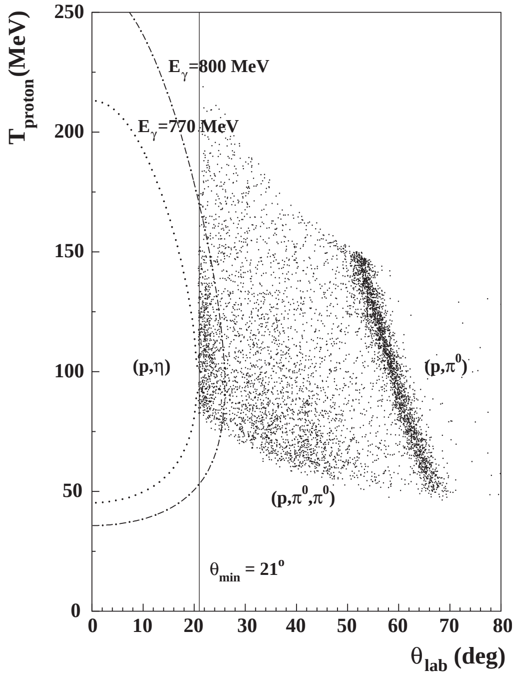

Fig. 1. The measured proton kinetic energy (T_{proton}) is shown as a function of the proton emission angle in the laboratory frame (θ_{lab}) for single charged events at $E_\gamma > 770$ MeV. The dotted and dash-dotted lines show the kinematical region allowed for the $p\eta$ reaction, respectively at $E_\gamma = 770$ MeV and $E_\gamma = 800$ MeV; the vertical line corresponds to the acceptance bound of DAPHNE.

2 Experimental setup

The experimental setup is described in detail in refs. [14, 16]. Only its main characteristics are briefly reviewed in the following. The experiment was carried out at the Glasgow-Mainz tagged-photon facility of the MAMI accelerator in Mainz. Circularly polarized photons were produced by bremsstrahlung of longitudinally polarized electrons. A strained GaAs photocathode routinely delivered electrons with a degree of polarization of about 75% [17]. The electron polarization was monitored with a precision of 3% by means of a Møller polarimeter. The photon polarization was evaluated according to ref. [18]. The photon energy was determined by the tagging spectrometer having an energy resolution of about 2 MeV [19]. The tagging efficiency was continuously monitored during the data taking by an e^+e^- pair detector installed downstream of the main hadron detector.

A butanol (C_4H_9OH) frozen-spin target [20] provided the polarized protons. The system consisted of a horizontal dilution refrigerator and a superconducting magnet ($\cong 2.5$ T), used in the polarization phase, together with a microwave system for dynamic nuclear polarization. During the measurement the polarization was maintained in the frozen-spin mode at a temperature of about 50 mK and a magnetic field of 0.4 T, supplied by a small superconducting holding coil inside the cryostat. The proton polarization was measured using NMR techniques with a precision of 1.6%. A maximum polarization close to 88% and relaxation times in the frozen-spin mode of about 200 h have been regularly achieved.

Photoemitted hadrons were registered in a large-acceptance detector DAPHNE [21]. DAPHNE is a charged-particle tracking detector covering the full azimuthal angular region and polar angles θ_{lab} from 21° to 159°. It consists of three cylindrical multiwire proportional chambers, surrounded by segmented plastic scintillator layers and by a scintillator-absorber sandwich. To increase the acceptance for the forward angular region, additional forward detectors, the silicon microstrip detector MIDAS [22], an aerogel Cerenkov counter to suppress electromagnetic background, and the annular ring detector STAR [23] were installed, followed by a forward scintillator-lead sandwich counter.

3 Data analysis

In this paper, data recorded using the DAPHNE detector alone are presented.

Events with a single charged track recognized as a proton were selected in order to identify the $p\eta$ channel. Due to this fact, only a small part of the reaction phase space is accessible, since in the measured photon energy range ($E_\gamma \leq 800$ MeV) protons are emitted with a maximum polar angle of $\simeq 25°$ and have enough energy to reach the detector only for $E_\gamma > 770$ MeV.

Protons were identified using the range method described in [24]. Its most important feature is the

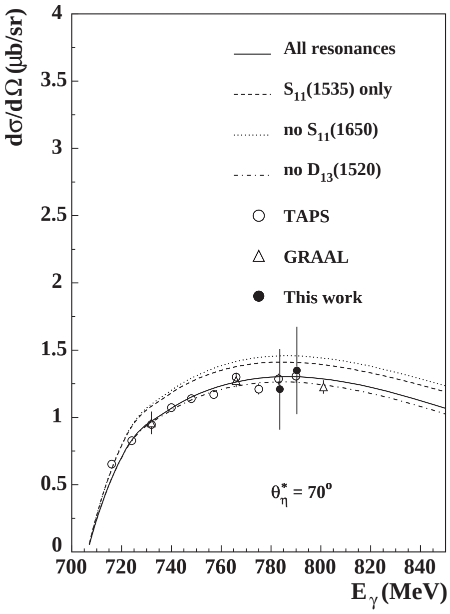

Fig. 2. The measured unpolarized excitation function at $\theta^*_\eta = 70°$ for the $\gamma p \to p\eta$ reaction (filled circles) is compared to the previously published data of ref. [1] (open circles) and ref. [3] (open triangles). The different style lines show the predictions of the MAID analysis for four different cases including all resonances (continuous line), $S_{11}(1535)$ only (dashed line), without $D_{13}(1520)$ (dash-dotted line), without $S_{11}(1650)$-resonances. The errors shown are statistical only.

simultaneous use of all of the charged-particle energy losses in the DAPHNE scintillator layers to discriminate between protons and $\pi^\pm$, and to determine their kinetic energies.

In fig. 1 the measured proton kinetic energy is shown as a function of the proton polar angle for events collected at $E_\gamma > 770$ MeV using an unpolarized pure-liquid-hydrogen target. The different regions where events coming from the $p\pi^0$, $p\pi^0\pi^0$ and $p\eta$ reactions show up, can be clearly seen. The dotted and dash-dotted lines show the kinematical region allowed for the $p\eta$ reaction at $E_\gamma = 770$ MeV and $E_\gamma = 800$ MeV, respectively. Events lying within the two lines were selected as possibly belonging to the $p\eta$ channel. While $p\eta$ and $p\pi^0$ reactions are clearly separated by the proton emission angle, events from the $p\pi^0\pi^0$ process extend into the kinematical region of the $p\eta$ production.

The background originating from the $p\pi^0\pi^0$ reaction has been evaluated by using a GEANT-based simulation and the known unpolarized $p\pi^0\pi^0$ cross-section [1,25]. The amount of this background is about 7% of the total selected events at $E_\gamma > 770$ MeV in the case of the unpolarized cross-section.

In fig. 2, the unpolarized excitation function at a center-of-mass angle $\theta^*_\eta = 70°$ and for E_γ between 780 MeV and 800 MeV is compared to previously published data [1] and the results of the multipole analysis MAID [26], which includes Born terms, vector meson exchange and nucleon resonances. The agreement suggests that both the detector response and the analysis method are well under control.

In the analysis of the data taken using the butanol target, the background contribution of the reactions on C and O nuclei could not be fully separated event by event from the polarized H contribution. However, this background, coming from spinless nuclei, is not polarization dependent and cancels when the difference between events in the 3/2 and 1/2 helicity states is taken. For this reason, only the helicity-dependent differential cross-section $\Delta\sigma_{13} = (\mathrm{d}\sigma/\mathrm{d}\Omega)_{1/2} - (\mathrm{d}\sigma/\mathrm{d}\Omega)_{3/2}$ can be directly extracted from the measurement with the butanol target. In this case, the helicity-dependent $p\pi^0\pi^0$ cross-section results of ref. [27] have been used for the background subtraction. The total number of remaining η events is 136 at 783 MeV and 111 at 798 MeV.

4 Results and discussion

By using the methods described above, the difference of the differential cross-sections $\Delta\sigma_{13} = (\mathrm{d}\sigma/\mathrm{d}\Omega)_{1/2} - (\mathrm{d}\sigma/\mathrm{d}\Omega)_{3/2}$ of η photoproduction was determined and is shown in fig. 3. Using our results of $(\mathrm{d}\sigma/\mathrm{d}\Omega)_{\mathrm{unpol}}$ (fig. 2), $(\mathrm{d}\sigma/\mathrm{d}\Omega)_{1/2}$ and $(\mathrm{d}\sigma/\mathrm{d}\Omega)_{3/2}$ were determined separately according to

$$(\mathrm{d}\sigma/\mathrm{d}\Omega)_{1/2} = (\mathrm{d}\sigma/\mathrm{d}\Omega)_{\mathrm{unpol}} + \Delta\sigma_{13}/2\,,$$
$$(\mathrm{d}\sigma/\mathrm{d}\Omega)_{3/2} = (\mathrm{d}\sigma/\mathrm{d}\Omega)_{\mathrm{unpol}} - \Delta\sigma_{13}/2\,.$$

The results are shown in fig. 3. The errors are statistical only. The systematic uncertainties contain contributions from charged-particle identification (2.5%), $\pi^0\pi^0$ background subtraction (1%), photon flux normalization (2%), photon polarization (3%), and target polarization (1.6%), respectively. The addition of these errors in quadrature leads to a total systematic error of about 6%. Due to the small acceptance of DAPHNE for detection of pure $p\eta$ events and the low statistics only one angular data point ($\theta^*_\eta = 70°$) for two γ energy bins can be given. In fig. 3 the predictions of the multipole analysis results of MAID [26] are also shown for four different cases including all resonances, for $S_{11}(1535)$ only, or switching off the $D_{13}(1520)$- or $S_{11}(1650)$-resonances.

These first measurements of the helicity-dependent differential cross-section $(\mathrm{d}\sigma/\mathrm{d}\Omega)_{1/2}$ for the $\vec{\gamma}\vec{p} \to p\eta$ reaction near threshold agree well with the MAID predictions. Also $(\mathrm{d}\sigma/\mathrm{d}\Omega)_{3/2}$ is small as expected for S-wave dominance near threshold. Clearly, better statistics and a wider kinematical range are required to disentangle the small contributions from resonances other than $S_{11}(1535)$. Analysis of the data from the more forward elements of the detector system (which is currently in progress) will extend the proton angle range down to 7.5° and will improve the statistics by a significative factor. In addition, data has been taken by our collaboration with a different experimental setup at ELSA (Bonn) which will cover the photon energy range up to about 1 GeV [28].

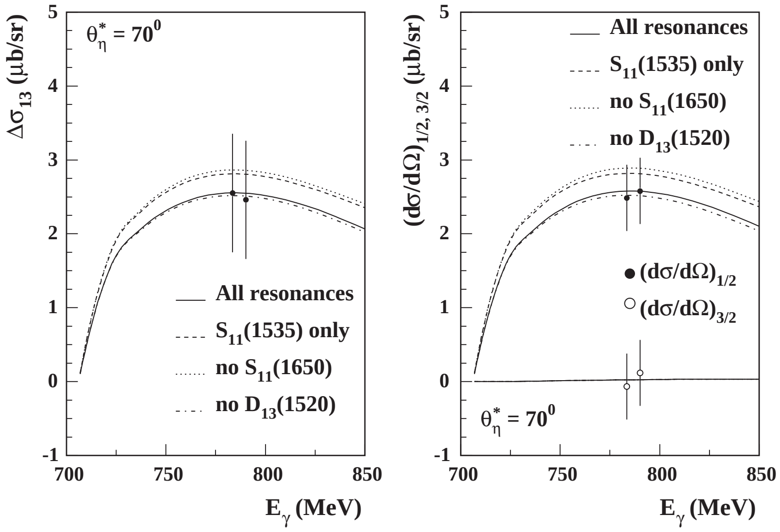

Fig. 3. The measured helicity-dependent differential cross-section for $\vec{\gamma}\vec{p} \to p\eta$. Left: $\Delta\sigma_{13} = (\mathrm{d}\sigma/\mathrm{d}\Omega)_{1/2} - (\mathrm{d}\sigma/\mathrm{d}\Omega)_{3/2}$. Right: $(\mathrm{d}\sigma/\mathrm{d}\Omega)_{1/2}$ and $(\mathrm{d}\sigma/\mathrm{d}\Omega)_{3/2}$. Curves as in fig. 2. The errors shown are statistical only.

We gratefully acknowledge the help and hospitality of the MAMI staff for providing excellent beam conditions and support. This work was supported by the Deutsche Forschungsgemeinschaft (SFB 201, SFB 443, Schwerpunktprogramm 1034, and GRK683), the INFN-Italy, the FWO Vlaanderen-Belgium, the IWT-Belgium, the UK Engineering and Physical Science Council, the DAAD, JSPS Research Fellowship, and the Grant-in-Aid (Specially Promoted Research) in Monbusho, Japan.

References

1. B. Krusche *et al.*, Phys. Rev. Lett. **74**, 3736 (1995).
2. A. Bock *et al.*, Phys. Rev. Lett. **81**, 534 (1998).
3. D. Rebreyend *et al.*, Nucl. Phys. A **663**, **664**, 436c (2000).
4. M. Dugger *et al.*, Phys. Rev. Lett. **89**, 222002 (2002).
5. G. Knoechlein, D. Drechsel, L. Tiator, Z. Phys. A **352**, 327 (1995).
6. B. Krusche, N.C. Mukhopadhyay, J.-F. Zhang, M. Benmerrouche, Phys. Lett. B **397**, 171 (1997).
7. C. Deutsch-Sauermann, B. Friman, W. Noerenberg, Nucl. Lett. B **409**, 51 (1997).
8. J. Denschlag, L. Tiator, D. Drechsel, Eur. Phys. J. A **3**, 171 (1998).
9. Z. Li, H. Ye, M. Lu, Phys. Rev. C **56**, 1099 (1997).
10. N. Kaiser, T. Wass, W. Weise, Nucl. Phys. A **612**, 297 (1997).
11. B. Borasoy, Eur. Phys. J. A **9**, 95 (2000).
12. L. Tiator, C. Bennhold, S.S. Kamalov, Nucl. Phys. A **580**, 455 (1994).
13. L. Tiator, D. Drechsel, G. Knoechlein, C. Bennhold, Phys. Rev. C **60**, 035210 (1999).
14. J. Ahrens *et al.*, Phys. Rev. Lett. **84**, 5950 (2000).
15. J. Ahrens *et al.*, Phys. Rev. Lett. **87**, 022003 (2001).
16. M. MacCormick *et al.*, Phys. Rev. C **53**, 41 (1996).
17. K. Aulenbacher *et al.*, Nucl. Instrum. Methods Phys. Res. A **391**, 498 (1997).
18. H. Olsen, L.C. Maximon, Phys. Rev. **114**, 887 (1959).
19. I. Anthony *et al.*, Nucl. Instrum. Methods Phys. Res. A **301**, 230 (1991); S.J. Hall *et al.*, Nucl. Instrum. Methods Phys. Res. A **368**, 698 (1996).
20. C. Bradtke *et al.*, Nucl. Instrum. Methods Phys. Res. A **436**, 430 (1999).
21. G. Audit *et al.*, Nucl. Instrum. Methods Phys. Res. A **301**, 473 (1991).
22. S. Altieri *et al.*, Nucl. Instrum. Methods Phys. Res. A **452**, 185 (2000).
23. M. Sauer *et al.*, Nucl. Instrum. Methods Phys. Res. A **378**, 143 (1996).
24. A. Braghieri *et al.*, Nucl. Instrum. Methods Phys. Res. A **343**, 623 (1994).
25. A. Braghieri *et al.*, Phys. Rev. Lett. B **363**, 46 (1995).
26. W.-T. Chiang, S.N. Yang, L. Tiator, D. Drechsel, Nucl. Phys. A **700**, 429 (2002).
27. F. Zapadtka, PhD Thesis, University of Göttingen, in preparation.
28. M. Godo, Diploma Thesis, University of Erlangen (2002).